nature nanotechnology

SUPPLEMENTARY INFORMATION

DOI: 10.1038/NNANO.2015.219

Identification of single nucleotides in MoS_2 nanopores

Jiandong Feng[1#], Ke Liu[1#], Roman D. Bulushev[1], Sergey Khlybov[1], Dumitru Dumcenco[2], Andras Kis[2], Aleksandra Radenovic[1*]

**correspondence should be addressed to aleksandra.radenovic@epfl.ch*

[#] equal contribution

COMSOL Modeling

Numerical calculations were performed using the COMSOL 4.2 multiphysics finite-element solver in 3D geometry, imposing a cylindrical symmetry along the axis of the nanopore. We solved the full set of Poisson–Nernst–Planck (PNP) equations, with the boundary conditions at the MoS_2 corresponding to an idealized, uncharged membrane impermeable to ions. The PNP set of equations extends Fick's law for the case where the diffusing particles/ions are displaced with respect to the fluid by the electrostatic force. Here we have expressed particle/ion concentrations in terms of mass fractions. In particular, all ion fluxes are modeled by the Nernst-Planck equation

$$\mathbf{J}_i = -D_i \nabla c_i - \frac{F z_i}{RT} D_i c_i \nabla \Phi \qquad (1.0)$$

where $\boldsymbol{J_i}$ and $\boldsymbol{D_i}$, are, respectively, the ion flux vector and diffusion coefficient of species i in the solution, T is the absolute temperature, Φ is the local potential, z_i is ionic charge and F Faraday´s constant. The relationship between the net electric charge of polyelectrolyte and local average electrostatic potential is described by the Poisson's equation.

$$\nabla^2 \Phi(r) = -\frac{\rho(r)}{\varepsilon} \qquad (1.1)$$

Both expressions can be rewritten using mass fractions

$$\begin{aligned} J_i &= -\rho D_i^F \nabla \varpi_i + \rho \varpi_i D_i^F \frac{\nabla M_n}{M_n} + D_i^T \frac{\nabla T}{T} + \rho \varpi_i z_i u_{m,i} F \nabla \Phi \\ M_n &= \left(\sum_i \frac{\varpi_i}{M_i} \right)^{-1} \end{aligned} \qquad (1.2)$$

where $\varpi_i = \frac{m_i}{\sum_i m_i}$ are the mass factors, ρ is the average density, M is the molar mass and $D^F{}_i$ are diffusion and $D^T{}_i$ thermal diffusion coefficients and *u* is the fluid velocity. In the case of 2M aqueous KCl solution (absence of the viscosity gradient), application of a fixed voltage generates the flux of K^+ and Cl^- ions that result in the net current that can be easily validated using the well-known analytical expression[1]

$$I = V\left(\left[\mu_{K^+} + \mu_{Cl^+}\right] n_{KCl} e\right)\left(\frac{4l}{\pi d^2} + \frac{1}{d}\right)^{-1} \quad (1.3)$$

where *V* is the applied voltage, n is the number density (proportional to concentration) of the ionic species, *e* is the elementary charge, and μ_{K+} and μ_{CL-} are the electrophoretic mobilities of the potassium and chloride ions, respectively. Parameter *d* represents the pore diameter and *l* is the membrane thickness. In the case of the viscosity gradient, the set of PNP equations has to be solved for 5 types of diffusing particles/ions subjected to the electrostatic force (4 ions and water molecules). Pore size was fixed to 2.5 nm, 5 nm and 10 nm (see, **Supplementary Fig. 1 (d-f)**). Simulated MoS_2 nanopore conductances, for all pore sizes in 2M aqueous KCl solution, viscosity gradient system or pure RT ionic liquid $BminPF_6$ were found to be in a good agreement with the measured values presented in **Supplementary Fig. (a-c).** In the case of the pure ionic liquid condition and for a fixed voltage, the resulting current originates from the flux of the $Bmim^+$ and PF_6^- ions.

DNA staining

DNA was stained with YOYO-1 as described elsewhere[2]. A 1 mM YOYO-1 stock solution (Invitrogen Y3601) was diluted in 10 mM sodium phosphate buffer (1.88 mM $NaH_2PO_4 \cdot H_2O$, 8.13 mM $Na_2HPO_4 \cdot 2H_2O$, pH 7.5) and mixed with λ-DNA with a ratio of 1 YOYO-1 molecule for 5 base pairs.

Theoretical model

In **Supplementary Fig. 4a** we schematize the free-energy surface with a well and a barrier to translocation for the case of our viscosity gradient system and for the 2M KCl aqueous solution. In the viscosity gradient system, λ-DNA adopts a random coil configuration with a gyration radius < 240 nm, while in the 2M KCl aqueous solution the corresponding gyration radius is ~570 nm (**Supplementary Fig. 5**). From the schematics, it is obvious that for both systems as long as the applied voltage is lower than the free energy barrier associated with the translocation process, one can expect low probabilities of translocations since they would only be driven by diffusion. On the other hand, increasing the applied voltage reduces the effective barrier and therefore significantly increases the probability of translocations. For the same pore, when working in the 2M KCl aqueous solution, we start to observe translocations at a much lower voltage of 100 mV compared to 200 mV when using the viscosity gradient system **Supplementary Fig. 4b.** This figure shows the comparison between translocation times for pNEB DNA for a wide range of applied voltages and two different electrolyte systems (2M KCl in H_2O and the viscosity

gradient system). According to Kramer's theory, DNA translocation governed by barrier in both systems obeys a power-law scaling,

$$\tau \sim e^{\left(\frac{\Delta G - qV}{k_B T}\right)} \tag{1.4}$$

where τ is dwell time, V the applied voltage, q effective charge and ΔG the height of the free-energy barrier. For both conditions, we observe an exponential dependence that reveals that translocation is voltage-activated, with typical events obtained at different voltages shown in **Supplementary Fig. 6.**

The Stokes drag force in the pores >5 nm

DNA-pore interactions can slow down DNA translocation in sub-5nm pores [3], while in the larger pores those interactions are negligible. Consequently, in the pores >5nm these interactions should not contribute to the DNA retardation. In the solution, long DNA molecules forms random coils, thus the viscous drag of the whole DNA molecule can be estimated as,

$$F_{drag} = 6\pi\eta v_{DNA} R_g \tag{1.5}$$

where R_g is the radius of gyration, η is the solvent viscosity, and v_{DNA} is the linear velocity of DNA translocation. As the polymer threads through the pore, the center of mass of this sphere moves toward the pore at a velocity:

$$v_{DNA} = \frac{dR_g}{dt} \tag{1.6}$$

Therefore, the Stokes drag force can be written as,

$$F_{drag} = 6\pi\eta_{IL} R_g \frac{dR_g}{dt} \tag{1.7}$$

If we assume that DNA translocation velocity is constant, this implies that the force balance between driving force and Stokes drag force is met at all times, *i.e.* from the first monomer translocation to the final monomer translocation.

Then, velocity can be expressed as:

$$v = \frac{R_g}{\tau} \tag{1.8}$$

where τ is the translocation time for the entire chain, denoted in experiments as the translocation dwell time. As proposed by Storm *et al.*[4], the principal effect of hydrodynamics is to resist motion with a hydrodynamic drag (Stokes drag) on the DNA coil.

$$F_{Drag} = F_{Driving} \tag{1.9}$$

In our case with water on both sides of the nanopore,

$$qE = 6\pi\eta R_g \frac{R_g}{\tau} \tag{1.10}$$

we obtain,

$$\tau = \frac{6\pi\eta}{qE} R_g{}^2 \tag{1.11}$$

Due to the fractal nature of DNA polymers, the equilibrium relation between R_g, the radius of gyration of the polymer and DNA length L_0 is best described by $R_g = L^{\nu}$. Then the expression 1.11 for the translocation time of the entire chain can be written as

$$\tau \sim \frac{6\pi\eta}{qE} L_0{}^{2\nu} \tag{1.12}$$

where ν is the Flory exponent.

For our viscosity gradient system, we only consider the biggest contribution to the Stokes drag force which originates form the drag of the DNA coil in the *cis* chamber since viscosity of RTIL is much higher than water.

Then,

$$F_{drag} = 6\pi\eta_{IL} R_g^{cis} \frac{dR}{dt} \tag{1.13}$$

where

$$R_g^{cis}(t) = \big((N-n)b\big)^{\nu} \tag{1.14}$$

where N is the total number of DNA monomers while *n* is the monomer number in the trans chamber and *b* corresponds the monomer length

$$F_{drag} = 6\pi\eta_{RTIL}(N-n)^{\nu} b^{\nu} \nu b^{\nu} (N-n)^{\nu-1} \frac{dn}{dt} \tag{1.15}$$

Introducing the force balance,

$$qE = 6\pi\eta_{RTIL}(N-n)^{\nu} b^{\nu} \nu b^{\nu} (N-n)^{\nu-1} \frac{dn}{dt} \tag{1.16}$$

$$\int_0^{\tau} qE dt = \int_0^{N} 6\pi\eta_{RTIL}(N-n)^{\nu} b^{\nu} \nu b^{\nu} (N-n)^{\nu-1} dn \tag{1.17}$$

For the viscosity gradient system, τ_{RTIL} chain translocation time can be written

$$\tau_{RTIL} \sim \frac{3\pi\eta_{IL} {L_0}^{2\nu}}{qE} \tag{1.18}$$

At this point we can introduce a retardation factor that allows us to compare between DNA translocation well times obtained aqueous 2M KCl solution in and in the viscosity gradient system

$$r = \frac{\tau_{RTIL}}{\tau_{H_2O}} = \frac{\eta_{RTIL}}{2\eta_{H_2O}} \tag{1.19}$$

We obtain a retardation factor higher than 140 that is predominantly due to the increase in the viscosity in our viscosity gradient system.

Translocated molecules	Length (bp, nt)	Supplier
Lambda	48502	New England Biolabs
Lambda HindIII	125, 564, 2027, 2322,4361, 6557, 9416 ,23130	New England Biolabs
pNEB 193, plasmid	2700	New England Biolabs
poly A30, T30, G30, C30	30	Microsynth
Single nucleotides	1	Sigma

Supplementary Table S1. DNA and nucleotides used in this work.

Supplementary References

1 Wanunu, M. *et al.* Rapid electronic detection of probe-specific microRNAs using thin nanopore sensors. *Nat Nanotechnol* **5**, 807-814, doi:Doi 10.1038/Nnano.2010.202 (2010).

2 Carlsson, C., Jonsson, M. & Akerman, B. Double Bands in DNA Gel-Electrophoresis Caused by Bis-Intercalating Dyes. *Nucleic Acids Res* **23**, 2413-2420 (1995).

3 Wanunu, M., Sutin, J., McNally, B., Chow, A. & Meller, A. DNA translocation governed by interactions with solid-state nanopores. *Biophys J* **95**, 4716-4725, doi:10.1529/biophysj.108.140475 (2008).

4 Storm, A. J. *et al.* Fast DNA translocation through a solid-state nanopore. *Nano Lett* **5**, 1193-1197, doi:Doi 10.1021/Nl048030d (2005).

5 Liu, K., Feng, J., Kis, A. & Radenovic, A. Atomically Thin Molybdenum Disulfide Nanopores with High Sensitivity for DNA Translocation. *Acs Nano* (2014).

FIGURES

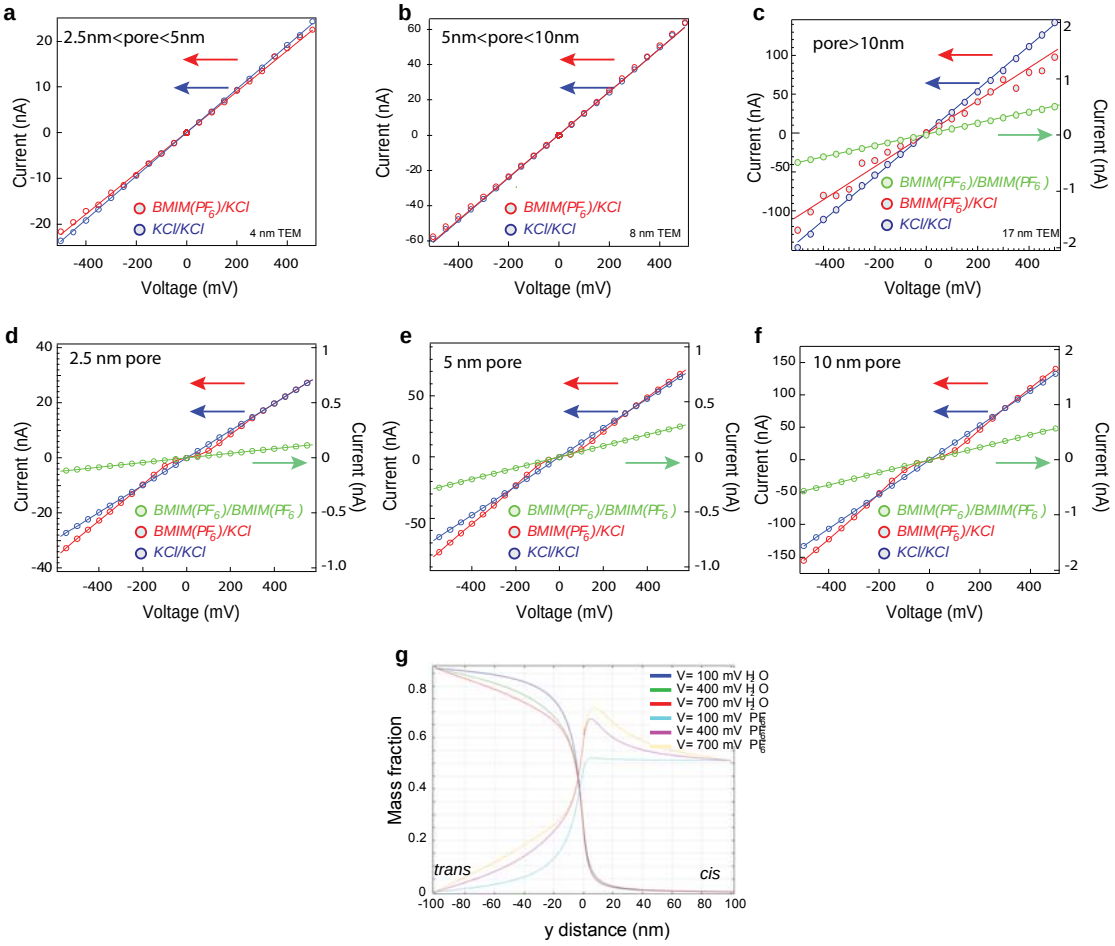

Supplementary Fig. 1. **Current-voltage characteristics of MoS_2 nanopores and COMSOL simulations of the ionic transport through a MoS_2 nanopore.** Measured current–voltage characteristics for viscosity gradient system (red), pure ionic liquid (green) and 2M aqueous KCl solution (blue) **(a)** in a pore smaller than 5 nm **(b)**, pore with a diameter between 5 nm and 10 nm **(c)** pore larger than 10 nm. Simulated current–voltage characteristics for a viscosity gradient system (red), pure ionic liquid (green) and 2M aqueous KCl solution (blue) in 2.5 nm pore having a conductance in gradient conditions of ~ 48 nS **(d),** 5 nm pore having conductance in gradient conditions of ~ 120 nS **(e)**, and 10 nm pore having conductance in gradient conditions of ~ 280 nS **(f)**. **(g)** Mass fraction as a function of distance from the nanopore center (marked as 0) of water, anions (PF_6^- and Cl^-), cations ($Bmim^+$ and K^+) at different applied voltages.

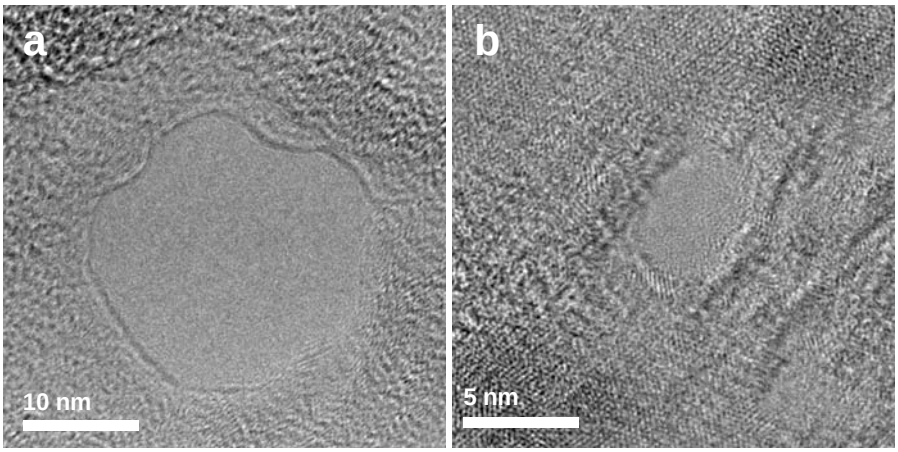

Supplementary Fig. 2. (a) High-resolution TEM images of a 22 nm diameter MoS_2 nanopore (data shown in Fig. 2) and a 2.8 nm diameter MoS_2 nanopore **(b)** (data shown in Fig.3 and 4) drilled using a focused electron beam. The same pore as in (a) has been used in Liu *et.al.* [5].

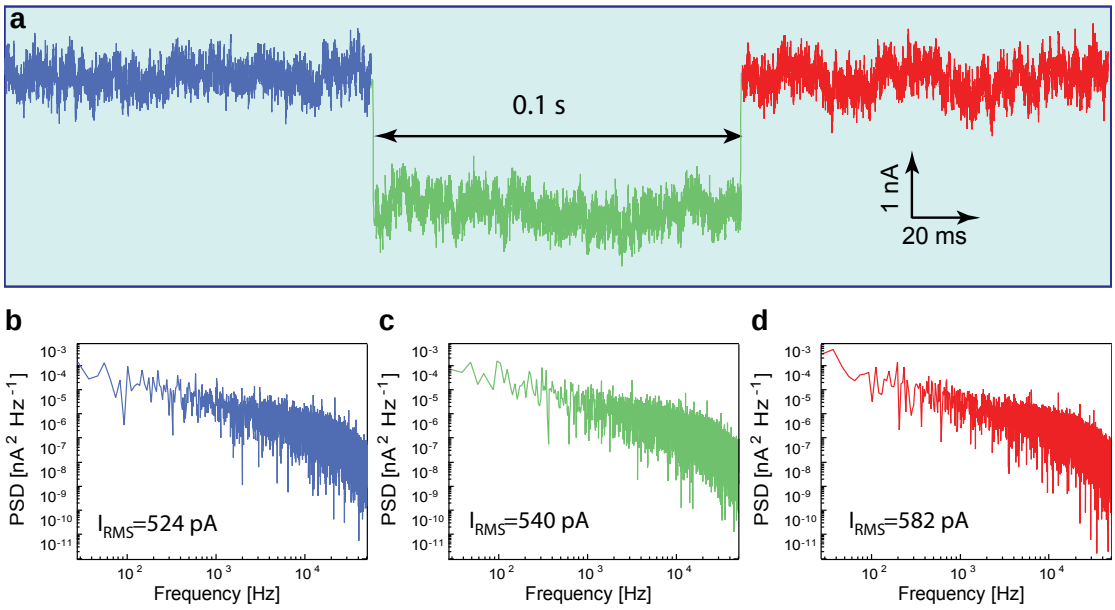

Supplementary Fig. 3. (a) An example of a 48.5 kbp λ-dsDNA translocation event in the viscosity gradient system. Current noise power spectra for the trace presented in **(a)** where the noise was calculated using Welch's method from 0.1 seconds of continuous data before DNA translocation (blue **(b)**) during (green **(c)**) and after (red **(d)**) DNA translocation.

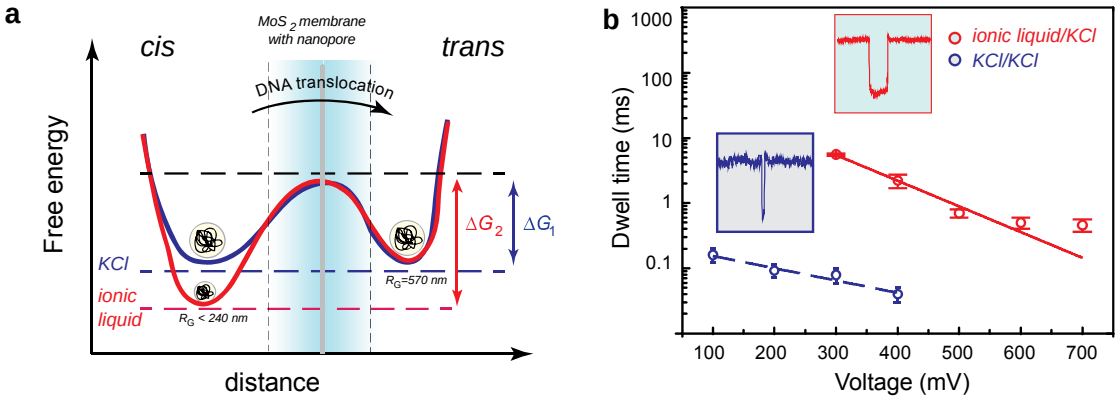

Supplementary Fig. 4. Single molecule DNA translocation through a nanopore probes the dynamics of Kramer's theory (a) Schematic representations of single-well free-energy surfaces, for two conditions. The schematics describes the intrinsic (i.e. zero voltage) free-energy surface with a well and a barrier to translocation. In the context of the voltage-driven translocation of individual DNA molecules in a nanopore, the well of the free-energy surface corresponds to the random-coil DNA configuration in a cis chamber with corresponding radius of gyration, while escape over the barrier involves translocation through the nanopore and subsequent adoption of the random-coil conformation. The free energy should include at least two parts, one from the phase transfer as described using L-J equation, another from the entropy part of the DNA coil. Both of these two energy parts give a similar phase as drawn, with the only significant difference being the distance and the free-energy level. **(b)** Dependence of the translocation dwell time on the applied voltage for pNEB DNA in ionic liquid/ KCl solution (red) and in KCl/KCl (blue). For both conditions, we observe an exponential dependence that reveals that translocation is voltage-activated. Blue and red lines are exponential fits to the data.

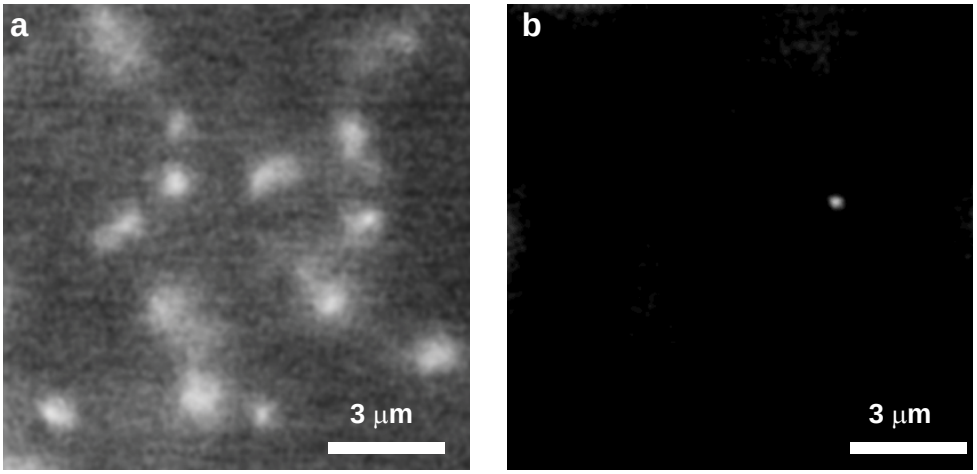

Supplementary Fig. 5. Fluorescence images of YOYO-1 labeled λ-DNA extracted from movies used to measure the diffusion coefficient of DNA in water **(a)** and **(b)** in RTIL ($BmimPF_6$). By tracking the locations of individual DNA molecules through a sequence of video frames, one can measure corresponding diffusion coefficients. Same movies were used to extract radius of gyration *Rg* of λ-DNA. In water it was ≈570 nm and less than 240 nm in $BmimPF_6$.

.

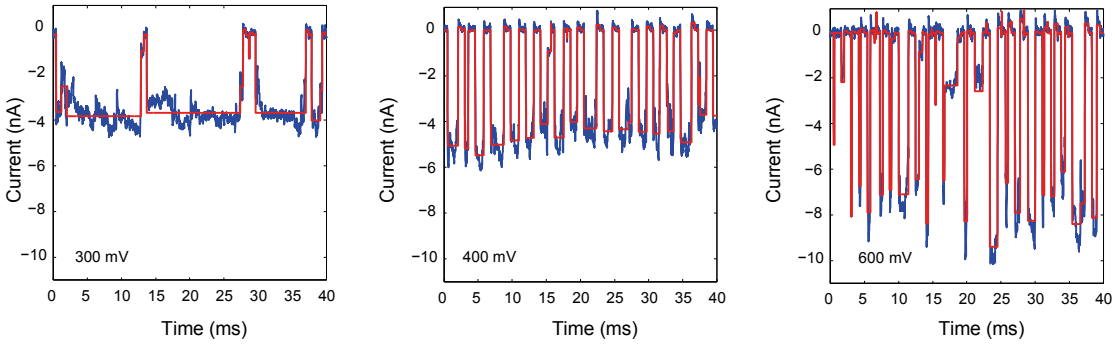

Supplementary Fig. 6. Example traces of pNEB translocation traces through a MoS_2 pore under ionic liquid/KCl condition with variable voltages (data used for **SI Fig. 4**). The most probable dwell times, from a single-exponential fit, are 5.5 ± 0.2 ms, 2.2 ± 0.5 ms, and 0.5 ± 0.1 ms for 300 mV, 400 mV, and 600 mV, respectively. This also shows a linear relationship between the current signal and applied voltage except at 500 mV (due to baseline fluctuation). We also observed enhanced signal under viscosity gradient conditions.

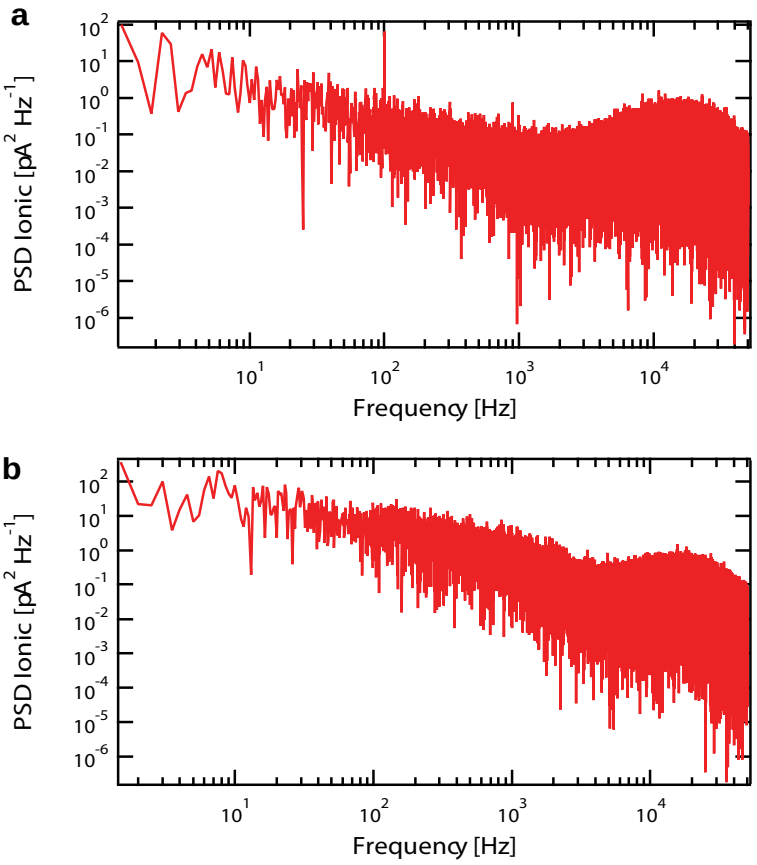

Supplementary Fig. 7. Current noise power spectra for the 3 nm diameter MoS_2 nanopore shown in SI Figure 1b). The noise was calculated using Welch's method from 1 second of continuous data before DNA translocation **(a)** at 0 m bias and (**b)** at 200 mV.

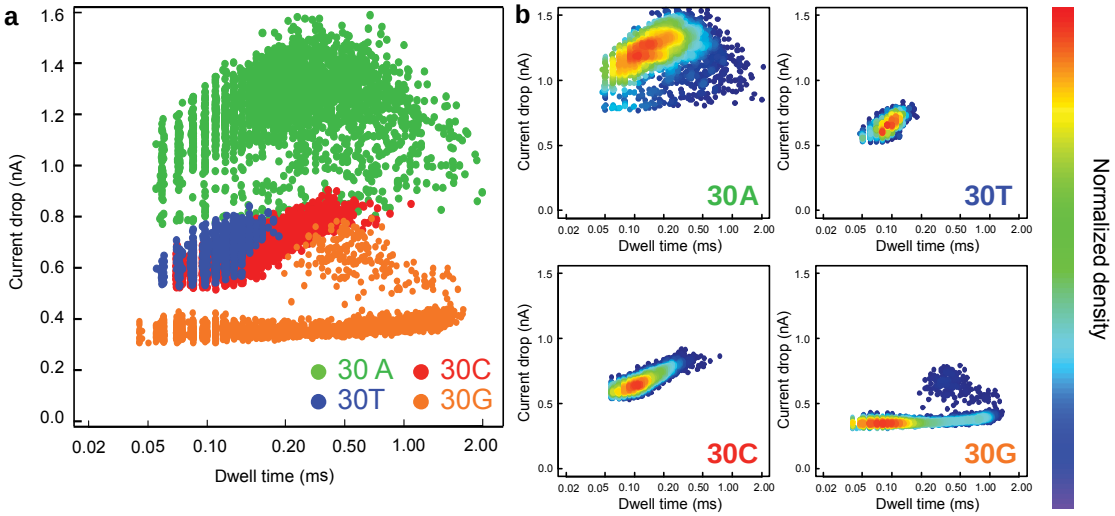

Supplementary Fig. 8. (a) Scatter plots of nucleotide translocation, showing distinguished current drops and dwell times for poly A30 (green), poly C30 (red), poly T30 (blue), and poly G30 (orange). b) Normalized histogram of current drops for each kind of the DNA homopolymer. The mean value for poly A30 is 1.25 nA, for poly C30 is 0.65 nA, for poly T30 is 0.7nA and for poly G30 is 0.45 nA. **(b)** Density plots of 30mer oligonucleotides in a MoS_2 nanopore; for poly A30, the position of the hot spot is (0.15, 1.25), for poly T30, (0.1, 0.75), for poly C30, (0.12. 0.65) and for poly G30 (0.09, 0.45). The color-map o the right shows the normalized density distribution of events. Data acquired for an experimental condition of pure RTIL in the cis chamber and 100 mM KCl, 25 mM Tris HCl, pH 7.5 in the trans chamber. The bias is +200 mV. The concentration of short DNA homopolymers in RTILs is 0.02 μmol/ml.

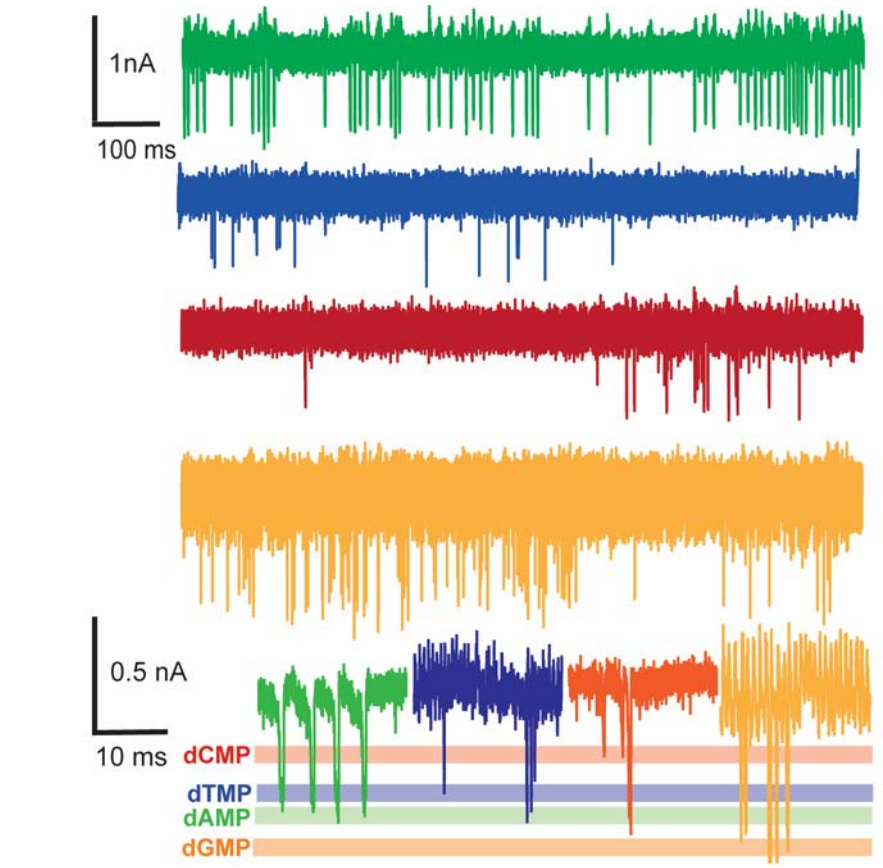

Supplementary Fig. 9. Differentiation of single DNA nucleotides in the 2.8 nm MoS_2 nanopore under ionic liquid/KCl gradient condition. 0.5 s and 0.1 s translocation signals for each nucleotide dAMP (green), dCMP (red), dTMP (blue), and dGMP (orange).

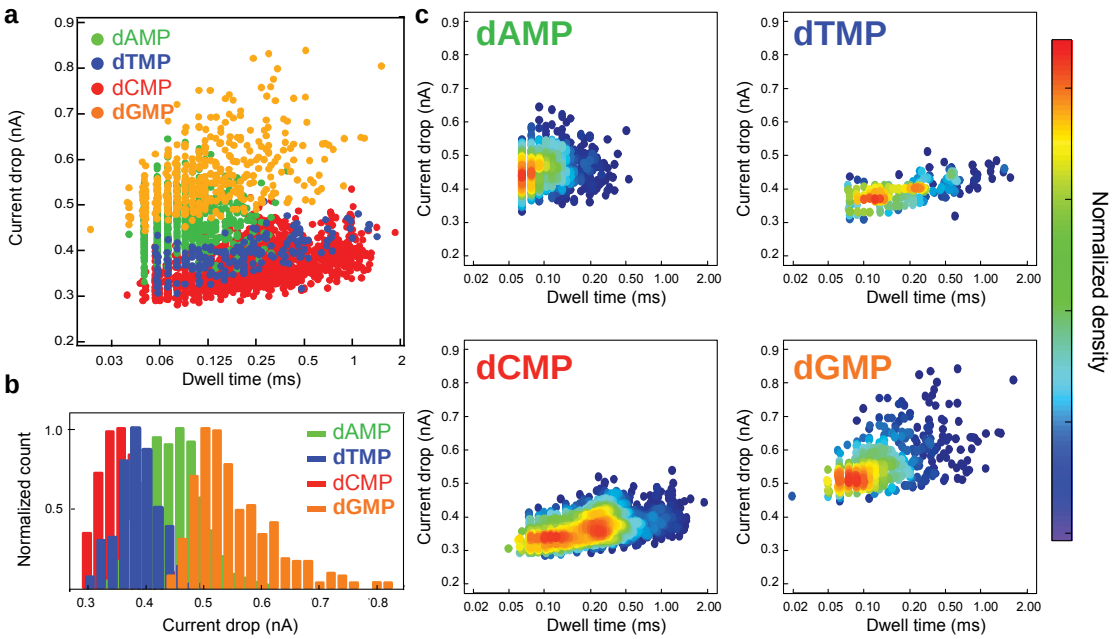

Supplementary Fig. 10. Identification of single nucleotides in a 3.3 nm MoS_2 nanopore. **(a)** Scatter plots of nucleotide translocation events, showing distinguished current drops and dwell times for dAMP (green), dCMP (red), dTMP (blue), and dGMP (orange). **(b)** Normalized histogram of current drops for dAMP, dTMP, dCMP, dGMP. **(c)** Density plot of single nucleotides in the MoS_2 nanopore; for dAMP, the position of the hot spot is (0.07, 0.46), for dTMP, (0.10, 0.40), for dCMP, (0.11. 0.36) and for dGMP (0.08, 0.56). The color-map at the right shows the normalized density distribution of events. It is clear that in the slightly larger pore nucleotide translocation events are faster and have smaller current amplitude drops. However, the trend of current drops for different types of nucleotides remains the same as shown in **Fig 4.** (dGMP>dAMP>dTMP>dCMP). Data acquired for an experimental condition of pure RTIL in the cis chamber and 100 mM KCl, 25 mM Tris HCl, pH 7.5 in the trans chamber. The bias is +200 mV. The nucleotide concentration in RTILs was 5μg/ml.

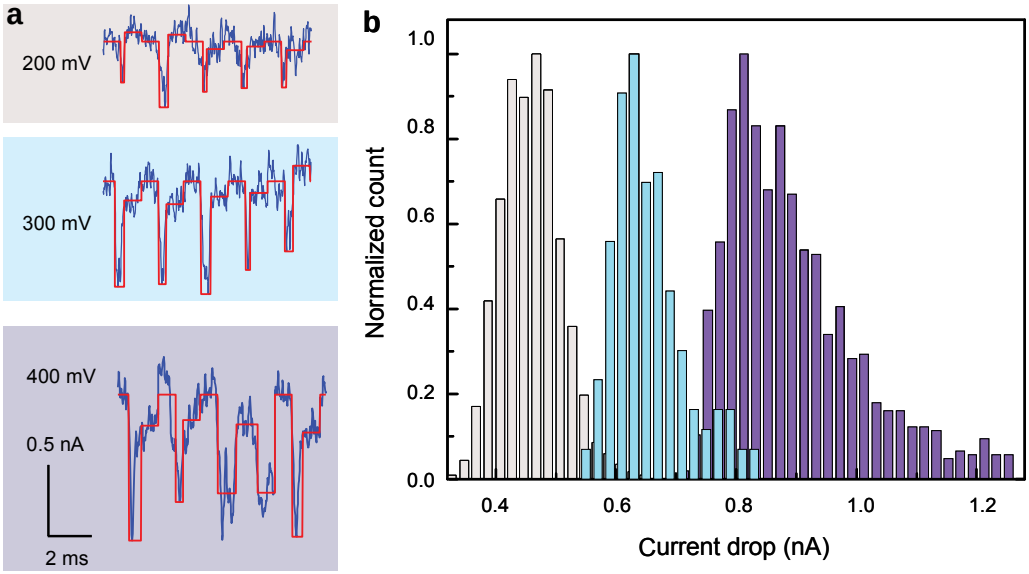

Supplementary Fig. 11. Example traces **(a)** and histograms **(b)** of dAMP translocation through a 3.3 nm MoS_2 pore in the presence of a viscosity gradient (ionic liquids/KCl), for different voltages (200 mV, 300mV and 400mV). The mean values for current drops are 0.46 nA, 0.65 nA, 0.91 nA, for 200 mV, 300mV, 400mV, respectively.

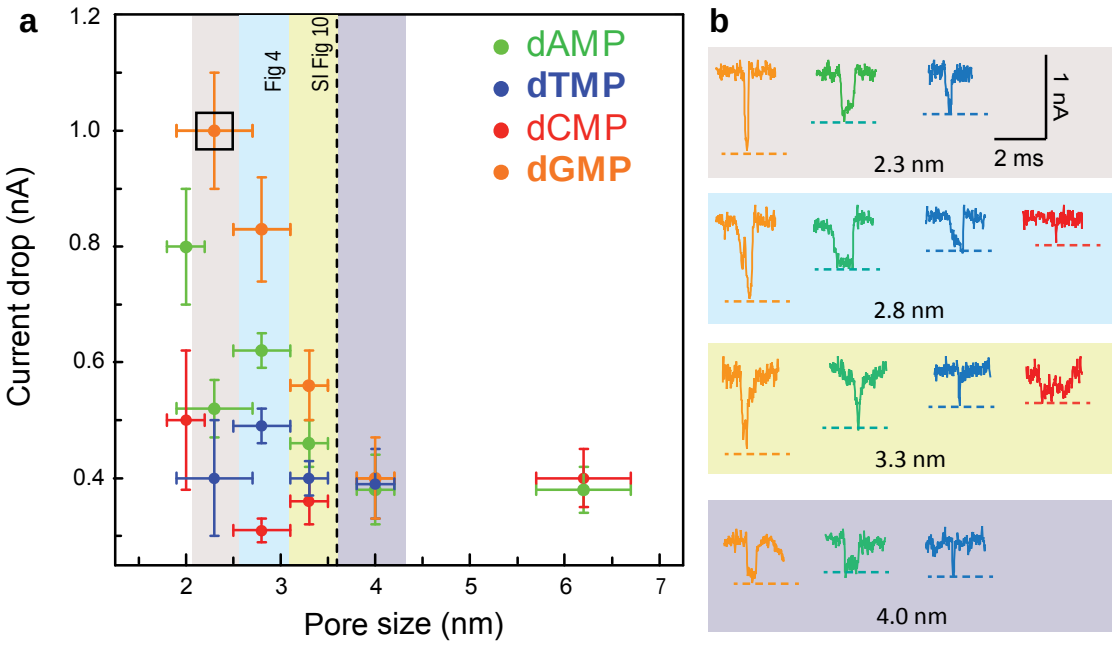

Supplementary Fig. 12. Pore size dependent differentiation/identification of four nucleotides based on ionic current drops. (a) Correlation between mean current drops of four nucleotides and pore sizes. Solid circles represent the experimentally determined mean current drops (standard deviation) for dAMP (green), dCMP (red), dTMP (blue), and dGMP (orange), respectively. Errors of pore sizes originate from the asymmetry of electron beam drilled pores. The black dashed line (around 3.6 nm) represents the maximum pore size that still allows differentiating between nucleotides. Nucleotides can be statistically identified within pores smaller than the critical size that is between 3.6 and 4 nm. Black rectangle indicates the data set with highest SNR (~16). **(b)** Typical events related to four nucleotides (labeled in color) translocating through MoS_2 nanopores with different diameters. The levels indicate the mean values for the current drops.